Numerical Modeling of Pneumatic Conveying in the Mode of the Inhibited Dense Layer

Asia. G. Mukhametzyanova, Andrei O. Pankov, and Alina A. Abdrakhmanova

Abstract Using the methods of computational fluid dynamics, we studied the process of pneumatic conveying in the mode of the inhibited dense layer. The results of numerical modeling correlate well with other scientists' data. The impact of the particle movement mode and shape of the arrestor is assessed on the stability of the process of pneumatic conveying in the mode of the inhibited dense layer.

Keywords Pneumatic conveying · Inhibited dense layer · Numerical modeling · Particle motion mode · Reliable conveying velocity

1 Introduction

Pneumatic conveying in the mode of the inhibited dense layer (IDL) is a perspective method of transporting bulk materials for short distances. These conditions allow to preserve the dense layer along the whole conveyor tube, and to get a high concentration of the solid phase in the flow, bringing its value to concentration in the stationary layer. To create an inhibited dense layer at the end of the conveyor tube conic narrowing parts with the conic angle of 1–2° are created, or arresters (diaphragm, cone head, etc.) are installed [1].

The properties that define pneumatic conveying in the mode of the inhibited dense layer are low consumption of the transported gas, the low conveying velocity with preservation of, system capacity in the solid phase, preservation of high concentration along the conveying tube, easiness of regulation of velocity of the bulk material flow

Asia. G. Mukhametzyanova (✉) · A. O. Pankov · A. A. Abdrakhmanova
Kazan National Research Technological University, Kazan 420015, Russia
e-mail: asia@kstu.ru

A. O. Pankov
e-mail: pankov.andrey@gmail.com

A. A. Abdrakhmanova
e-mail: abdrakhmanova.alina93@yandex.ru

A. G. Kravets et al. (eds.), *Society 5.0: Cyberspace for Advanced Human-Centered Society*, Studies in Systems, Decision and Control 333,
https://doi.org/10.1007/978-3-030-63563-3_14

over a broad area, etc. [2]. One of the main advantages of pneumatic conveying in the mode of inhibited dense layer is the opportunity to combine with other technological processes, such as cleaning from light impurities with pneumatic separators, drying with the stream of the warmed gas, catalysis, pyrolysis, etc. [3].

Application of pneumatic conveying in the mode of the inhibited dense layer could be quite useful in many cases for solving a whole range of technological problems. The main problem for the performance of pneumatic conveying in the mode of inhibited dense layer is lack of studies, lack of impression of the structure of the inhibited dense layer, and impact on it of various technological, structural, and mode's parameters.

The reliability and economic feasibility of pneumatic conveying depend on the right choice of the airflow velocity. The increase of this velocity reduces the operational life of pneumatic pipes, leads to an increase of pressure loss in the network, and electrical power consumption, and its reduction causes fallout of the transported material in the pneumatic pipe and blockage of the latter. The right choice of the velocity of the transporting gas is extremely important both for sustainable conveying mode and for energy efficiency.

Controlling influence over speed of the material in pneumatic conveying in the mode of the inhibited dense layer has a hydrodynamic environment created in the braking area. Moreover, the concentration of the material transferred in the airflow also affects transportation speed [4]. Work [5] shows that the speed of the bulk material in the mode of the inhibited dense layer depends on the physical-mechanical properties of the granular material, gas speed, dimensions, and form of the narrowing arrester and does not depend on the length and unevenness of the transport pipe.

2 Background and Problem Statement

The reliable transporting speed should be higher than the engulfment velocity. This velocity may be in large excess over the first velocity of pseudo-fluidization in usual modes of pneumatic conveying and may be almost the same as the terminal velocity of the particles (the second critical velocity of pseudo-fluidization).

In course of pneumatic conveying in the mode of inhibited dense layer movement of the particles is restricted so much that terminal velocity becomes much lower and engulfment velocity becomes almost the same as the first velocity of pseudo-fluidization. The extension of the layer during pneumatic conveying is not large, its structure is almost the same as of the solid phase of the fluidized state. Therefore, gas speed should be a few times higher than the velocity at the beginning of the pseudo-fluidization of the transported material. In this case, we mean gas velocity in the lower part of the conveying tube. While moving up in the transport pipe the gas velocity increases due to its extension, bearing capacity increases, and engulfment hazard is excluded.

The process of the established pneumatic conveying of solid spherical particles along the smooth vertical part of the pipe is studied herein with methods of computational fluid dynamics. STAR-CCM + computational complex was used as the studies instrument, that allows obtaining solutions for a wide range of physical problems, including for transient circuits, coupled heat transfer, exposure, laminar, and turbulent frictional flow, etc.

The approach to the modeling of movement of two-phase flows is majorly determined by the intensity of mutual interaction and depends on the volume ratio of the solid phase in a flow [6–8].

If the volume ratio of solid particles is less than 10–6, the particles do not affect the movement of the gas flow. If the volume ratio of solid particles is increased to 10–3, the interaction between the gas and the particles is observed, however, the movement of separate particles is regarded to be independent of each other [6]. In the case of higher concentrations of solid particles interaction between the particles in a flow is observed, as well as between the particles and the device walls that lead to changes of movement of the gas phase.

In course of studies of fluid dynamics of two-phase flows, a few model approaches that differ from each other by the method of review of the interacting phases and link between them are formulated and clarified.

The work [9] provides a classification of imitation models depending on the area of their application and description of the interaction of the phases.

According to the authors [8–17], the most practical bearing for modeling of the weighted layer has the model of discrete elements and the continuous model, the principal difference between which is the description of the movement of the discrete particles, and the common problem is the preparation of the closing relations, and, particularly, determination of the mechanical interaction of the phases.

Movement of the gas phase for discrete element model or Eulern-Lagrangian model is solved in Euler representation, as a continuum in an immovable coordinate system, and movement of particles is represented with Lagrangian equations in the movable coordinate system that are integrated along their trajectory [6, 8].

The model of discrete elements, which is solved by integration of the particle movement equations within the velocity field of the bearing gas, allows obtaining statistical data on the movement of the separate particles with regard to their density, dimensions, shape, and polydispersity of the particles [6].

However, frequent application of the model of discrete particles in full for large concentrations of particles is restricted due to complexity and long term of computations made in a few iterations [13, 14].

3 Numerical Modeling

For the purposes of studies of two-phase flows, particularly, of the gas-solid particles flow STAR-CCM + computational complex provides for the Lagrangian multiphasicity model and Discrete Element Method—DEM.

For numerical modeling of two-phase gas-solid particles flow Discrete Element Method—DEM was applied, that allowed to design clashes of particles of any shape and to consider gyration of the particles affected by the forces and their moments.

Discrete Element Method DEM is a set of numerical methods for the design of a large number of particles of solid materials. The key provision of the method is, that the material is comprised of separate discrete particles, that may have various properties and surface shapes, elastic properties, density, etc.

Modeling starts with moving of all of the particles to a specific position and assignment to them of the initial speed. Then the forces affecting every particle are calculated by the initial data and the relevant physical laws. For every particle dynamic problem is solved that includes determination of the active forces and movement trajectory [17].

For calculation of the terminal velocity of solid spherical particles in a vertical pneumatic conveying system of three-dimensional Navier–Stokes equations, averaged by Reynolds (Formulas 1–7) is solved, supplemented with discrete methods based on the Lagrangian approach.

Airflow is described as follows:

- mass preservation equation

$$\overline{\mathrm{V}}(\overrightarrow{\mathrm{V}}) = 0 \tag{1}$$

- impulse preservation equation

$$\frac{\partial \vec{V}}{\partial t} + \bar{V}(\vec{V}\vec{V}) = -\frac{\nabla p}{\rho} + \frac{\nabla\left(\overline{\overline{\tau}} + \overline{\overline{\tau_t}}\right)}{\rho}; \tag{2}$$

viscous tensor $\overline{\overline{\tau}}$ is determined with Newton rheological law:

$$\overline{\overline{\tau}} = \mu * (\nabla \overrightarrow{\mathrm{V}} + [\nabla \overrightarrow{\mathrm{V}}]^{\mathrm{T}}) - \frac{2}{3} * \mu \nabla * \overrightarrow{\mathrm{V}} * \overline{\overline{\mathrm{I}}}, \tag{3}$$

and Reynolds stress tensor $\overline{\overline{\tau_t}}$—in accordance with the generalized hypothesis by Boussinesq:

$$\overline{\overline{\tau_t}} = \mu_{\mathrm{t}} * (\nabla \overrightarrow{\mathrm{V}} + [\nabla \overrightarrow{\mathrm{V}}]^{\mathrm{T}}) - \frac{2}{3} * \mu_{\mathrm{t}} \nabla * \overrightarrow{\mathrm{V}} * \overline{\overline{\mathrm{I}}} - \frac{2}{3} * \rho * k * \overline{\overline{\mathrm{I}}}. \tag{4}$$

To determine turbulence specifications $-\ \varepsilon$ turbulence model was applied:

$$\frac{\partial}{\partial \mathrm{t}}(\rho * k) + \nabla[\rho * \overrightarrow{V} * k - (\mu + \frac{\mu_t}{\sigma_{\mathrm{k}}} * \nabla] = \mu_{\mathrm{t}} * \mathrm{P} - \rho * \varepsilon, \tag{5}$$

$$\frac{\partial}{\partial t}(\rho * \varepsilon) + \nabla[\rho * \overrightarrow{V} * \varepsilon - (\mu + \frac{\mu_t}{\sigma_\varepsilon} * \nabla\varepsilon] = C_{\varepsilon 1} * \frac{\varepsilon}{k} * -\mu_t * P - C_{\varepsilon 2} * \frac{\varepsilon^2}{k}; \quad (6)$$

Generation component in transfer equations

$$P = \mu * (\Delta\overrightarrow{V} + [\Delta\overrightarrow{V}]^T) * \Delta\overrightarrow{V}, \quad (7)$$

where —turbulence kinetic power; ε—turbulence kinetic power velocity; μ_t—turbulence viscosity; $C_{\varepsilon 1}$, $C_{\varepsilon 2}$—semiempirical ratios of turbulence model.

General equation of impulse preservation for the material particle as follows

$$m_p = \frac{dv_p}{dt} = F_s + F_b; \quad (8)$$

where F_s—forces affecting the particle surface; F_b—mass forces affecting the particle. These forces, in their turn, divide into

$$F_s = F_d + F_p; \quad (9)$$

$$F_b = F_g + F_c; \quad (10)$$

where F_d—resistance force; F_p—tensile force; $F_g = m_p g$—gravitational force; F_c—additional forces of the body that are represented by the interaction of the particles with other particles and boundaries of the area. At that, F_c is represented as follows

$$F_c = \Sigma_{neighbor.particles} F_{contact} + \Sigma_{neighbor.boundaries} F_{contact}; \quad (11)$$

In addition to impulse preservation equation (8), the discrete element model includes an equation for computation of the particles turn:

$$\frac{d}{dt}L_p = \frac{d}{dt}(I_p\omega_p) = \Sigma_{neighbor.particles} T_c + \Sigma_{neighbor.particles} T_A; \quad (12)$$

where the torque is calculated as follows

$$T_c = r_c F_c - \mu_r |r_c||F_c| \frac{\varpi_p}{|\varpi_p|}; \quad (13)$$

where L_p—angular moment of the particle; I_p—inertia moment of the particle; T_c—torque of the separate particle that occurs as a result of the operation of the exchange forces, applied to the particle in the point other than the particle center of mass; r_c—vector from the center of mass to contact point; μ_r—coefficient of rolling friction; ϖ_p—the angular spin rate of the particle. The coefficient of rolling friction is determined during verification with the experimental model and is set as 0.3. Force in (9) and (10) are modeled as follows.

The equation for tensile force F_d

$$F_d = \frac{1}{2} C_d \rho A_p |\nu_s| \nu_s; \tag{14}$$

where C_d—coefficient of rolling friction; ρ—air density; ν_s—slide speed of the particle; A_p—projected area of the particle.

The equation for tensile force F_p

$$F_p = -V_p \nabla p_{static}; \tag{15}$$

where V_p—particle volume; $\nabla_{P_{static}}$—static pressure gradient of the basic phase.

For a description of the interaction between $F_{constant}$ particles Hertz-Mindlin interaction model was used that is based on the Hertz-Mindlin interaction theory.

Pursuant to this model the forces affecting between these two spheres A and B are described by the following group of the equations.

$$F_{contact} = F_n + F_t; \tag{16}$$

where F_n—normal and F_t—tangential forces.

Normal force:

$$F_n = -K_n d_n - N_n \nu_n; \tag{17}$$

where $K_n = \frac{3}{4} E_{eq} \sqrt{d_n + R_{eq}}$—normal spring tension; $N_n = \sqrt{(5K_n M_{eq})} N_{n\,damp}$—normal damping; $N_{n\,damp}$—normal decay coefficient, determined by the Eq. (20).

Tangential force is determined as follows

$$F_t = -K_t d_t - N_t \nu_t; \tag{18}$$

if $|K_t d_t| < |K_n d_n| C_{fs}$;

$$F_t = \frac{|K_n d_n| C_{fsd_t}}{|d_t|}; \tag{19}$$

$|K_t d_t| \geq |K_n d_n| C_{fs}$,

where C_{fs}—coefficient of static friction, tangential spring tension $K_t = 8G_{eq}\sqrt{d_n R_{eq}}$, tangential damping; $N_t = \sqrt{(5K_t M_{eq})} N_{t\,damp}$, $N_{t\,damp}$—tangential decay coefficient, determined by Eq. (21)

$$N_{n\,damp} = \frac{-\ln(C_{n\,rest})}{\sqrt{\pi^2 + \ln(C_{n\,rest})^2}}; \tag{20}$$

$$N_{t\,damp} = \frac{-\ln(C_{t\,rest})}{\sqrt{\pi^2 + \ln(C_{t\,rest})^2}}; \tag{21}$$

where $C_{n\,rest}$ and $C_{t\,rest}$—normal and tangential elasticity coefficient; R_{eq}, M_{eq}, E_{eq}, G_{eq}—equivalent radius of particles, Young's modulus, shear modulus correspondingly.

As initial data were taken physical parameters of the air under normal conditions, input, and output velocity. Configurations are set for the interaction of the particles with each other and with walls of the computational region.

The problem for setting the movement of the traffic flow in a rectangular channel with a diameter of 0.02 m and length of 2.2 m. Spherical particles with a diameter of 0.003 are taken. Change of modes (transfer from the inhibited dense layer to piston flow) was determined according to output pressure pulsation—in the mode of an inhibited dense layer, this parameter does not exceed 10% [18].

Numerical modeling of the movement process of two-phase flow along the conveying tube allowed to detect velocity fields of both of the phases, pressure, and other values. The results of numerical modeling correlate well with other scientists' data [2]. The impact of the particle movement mode and shape of the arrestor is assessed (Fig. 1) on the stability of the process of pneumatic conveying in the mode of an inhibited dense layer, minimum gas velocities for transportation of the bulk materials in various conditions are determined.

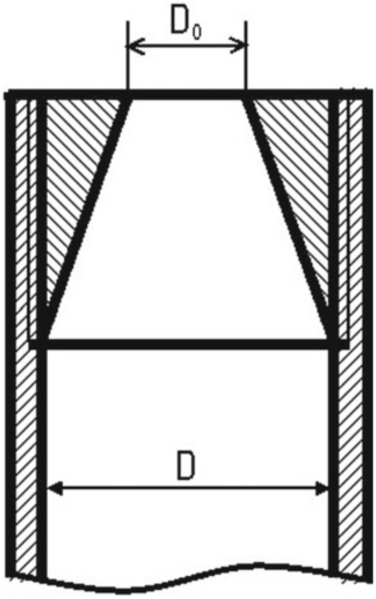

Fig. 1 Example of the controller (arrestor)

4 Results and Discussion

The following values varied in the numerical experiments: compression rate D0/D; conveying tube diameter D; density of the transported materials (in Table 1 it is implicitly expressed by the first velocity of pseudo-fluidization).

Analysis of the results of numerical modeling shows that the value of the minimum gas velocity during pneumatic conveying of bulk materials in the mode of inhibited dense layer is 30–70% higher than the velocity at the beginning of pseudo-fluidization. The velocity at the beginning of pseudo-fluidization was determined in accordance with Todes formula [19].

An increase of simplex D0/D (that is the reduction of the compression level) leads to the growth of the minimum gas velocity. A maximum increase occurs upon achievement of the critical values D0/D, which are the values when the mode of inhibited dense layers transfers to piston pneumatic transport. The maximum value of this increase amounts to 50–100%, and the upper limit may be regarded as reliable conveying gas velocity.

The results of numerical modeling show that the increase of conveying tube diameter causes a reduction of the minimum velocity value. Apparently, this can be explained by the fact that tubes of smaller diameter are more prone to piston formation. Therefore, the tubes of larger diameter ensure a more stable process, and a stationary mode of transportation is established earlier.

Table 1 Results of numerical modeling of pneumatic conveying of bulk materials in the mode of the inhibited dense layer in various conditions

Pseudofluidization velocity (m/s)	Conveying tube diameter, $D * 10^2$ m	Minimum conveying velocity (m/s)		Pseudofluidization number		Reliable conveying velocity (m/s) (comp.)
		Maximum inhibition	Minimum inhibition	Maximum inhibition	Minimum inhibition	
0.215	15	0.29	0.41	1.35	1.90	0.46
0.334	15	0.51	0.60	1.52	1.80	0.71
0.104	16	0.17	0.21	1.61	2.04	0.23
0.104	28	0.17	0.19	1.66	1.84	0.19
0.118	16	0.16	0.18	1.39	1.54	0.23
0.118	28	0.17	0.18	1.42	1.50	0.27
0.118	40	0.17	0.22	1.47	1.87	0.26
0.373	28	0.50	0.59	1.34	1.58	0.73
0.370	40	0.59	0.66	1.57	1.77	0.73
0.531	28	0.74	0.90	1.40	1.70	0.97
0.531	40	0.71	0.77	1.34	1.45	0.98

5 Conclusion

Thus, we can conclude that for the purposes of determination of the minimum allowable velocity of pneumatic conveying of the bulk materials it is necessary to carry out numerical experiments for specific terms, and unless it is possible to carry out numerical computations, this velocity shall be equal to the doubled value of the first velocity of pseudo-fluidization.

References

1. Li, Hongzhong: Mooson Kwauk. Chem. Eng. Sci. **44**(2), 261–271 (1989)
2. Razinov Y.I.: Study of vertical pneumatic conveying of bulk materials with inhibited dense layer. Dissertation Thesis for Ph.D. in Engineering (Candidate of Engineering Sciences), p. 212. Kazan (1974) (in Russian)
3. Mills, D., Jones, M.G., Agarwal, V.K.: Handbook of Pneumatic Conveying Engineering, p 720. CRC Press (2004)
4. Yu, M.A.: Numerical modeling of impact of the air flow on spherical particles in the round-section air duct. In: Modern Issues of Science and Education. No. 2 (part 2), pp. 107–113 (2015)
5. Yu, M.A., Kolosnitsin, A.N.: Development of numerical methods of vacuum cleaning system design. Herald of Civil Engineers **6**(59), pp. 151–155 (2016)
6. Klinzing, G.E., Rizk, F., Marcus, R., Leung, L.S.: Pneumatic Conveying of Solids. A Theoretical and Practical Approach, p. 435. Springer (2010)
7. Yu, V.A.: Turbulentnye techeniya gaza s tverdymi chasticami [Turbulent Flows of Gas with Solid Particles], 192 p. Moscow, Fizmatlit (2003) (in Russian)
8. Ostrovsky G.M.: Pnevmoticheskiyi transport sypuchih materialov v himicheskoyi promyshlennosti [Pneumatic Transport of Loose Materials in the Chemical Industry], 104 p. Lenin-grad, Khimiia (1984) (in Russian)
9. Schreiber, M.: Modellierung von Hydrodynamik und Wärmeübertragung in blasenbildenden Wirbelschichten zur Trocknung von Braunkohle: akademischen Grades eines Doktor-Ingenieurs genehmigte Dissertation. Brandenburgischen Technischen Universität Cottbus, 167 p (2013)
10. van der Hoef, M.A., van Sint Annaland, M., Deen, N.G., Kuipers, J.A.M.: Numerical Simulation of Dense Gas-Solid Fluidized Beds: A Multiscale Modeling Strategy. Annual Review of Fluid Mechanics, vol. 40, pp. 47–70 (2008)
11. van der Hoef, M.A., Ye, M., van Sint Annaland, M., Andrews, A.T., Sundaresan, S., Kuipers, J.A.M.: Multiscale modeling of gas-fluidized beds. Adv. Chem. Eng. **31**, 65–149 (2006)
12. Elghobashi, S.: Particle-Laden turbulent flows. Direct simulation and closure models. Appl. Sci. Res. **48**, 301–314 (1991)
13. Flow Simulation 2014 Technical Reference. Dassault Systems, 204 p (2014)
14. Gui, N., Fan, J.R., Luo, K.: DEM-LES study of 3-D bubbling fluidized bed with immersed tubes. Chem. Eng. Sci. **63**(14), 3654–3663 (2008)
15. Chiesa, M., Mathiesen, V., Melheim, J.A., Halvorsen, B.: Numerical simulation of particulate flow by the Eulerian-Lagrangian and the Eulerian-Eulerian approach with application to a fluidized bed. Comput. Chem. Eng. **29**(2), 291–304 (2005)
16. Gidaspow, D., Ettehadieh, B.: Fluidization in two-dimensional beds with a jet—2 hydrodynamic modeling. Ind. Eng. Chem. Fundam. **22**(2), 193–201 (1983)
17. Gidaspow, D.I.: Multiphase flow and fluidization continuum and kinetic theory descriptions, p. 467. Academic Press Harcourt Brace & Company, San Diego (1994)

18. Mukhametzyanova, A.G., Pankov, A.O., Abdrakhmanova, A.A.: Selection of Criteria of Pneumatic Conveying in the Mode of Inhibited Dense Layer, vol. 22, No. 10, pp. 72–76. Herald of Engineering University (2019)
19. Yu, V.V., Belova, O.V., Skibin, A.P., Zhuravlev, O.N.: Determination of Fluid Dynamic Performance of Restrictor with Labyrinth Sealing Using Computational Fluid Dynamics, pp. 55–64. Herald of the Bauman Moscow State Technical University (2012)